International Journal of Biological Macromolecules 162 (2020) 1869–1879

Contents lists available at ScienceDirect

International Journal of Biological Macromolecules

journal homepage: http://www.elsevier.com/locate/ijbiomac

Anti-staphylococcal hydrogels based on bacterial cellulose and the antimicrobial biopolyester poly (3-hydroxy-acetylthioalkanoate-*co*-3-hydroxyalkanoate)

Virginia Rivero-Buceta [a,e], María Rosa Aguilar [b,c,e,*], Ana María Hernández-Arriaga [a,e], Francisco G. Blanco [a,e], Antonia Rojas [d,e], Marta Tortajada [d,e], Rosa Ana Ramírez-Jiménez [b,c,e], Blanca Vázquez-Lasa [b,c,e], Auxiliadora Prieto [a,e,*]

[a] Polymer Biotechnology Group, Biological Research Center (CIB-CSIC), CSIC, 28040 Madrid, Spain
[b] Biomaterials Group, Institute of Polymer Science and Technology (ICTP-CSIC), Spain
[c] Networking Biomedical Research Centre in Bioengineering, Biomaterials and Nanomedicine (CIBER-BBN), Spain
[d] ADM-Biopolis Parque Científico Universidad de Valencia, edf. 2 C/Catedrático Agustín Escardino, 9, 46980 Paterna, Valencia, Spain
[e] Interdisciplinary Platform for Sustainable Plastics towards a Circular Economy-Spanish National Research Council (SusPlast-CSIC), Madrid, Spain

ARTICLE INFO

Article history:
Received 15 April 2020
Received in revised form 23 July 2020
Accepted 26 July 2020
Available online 07 August 2020

Keywords:
Bacterial cellulose
Polyhydroxyalkanoates
Antimicrobial polyester

ABSTRACT

Polymeric hydrogels from bacterial cellulose (BC) have been widely used for the development of wound dressings due to its water holding capacity, its high tensile strength and flexibility, its permeability to gases and liquids, but lacks antibacterial activity. In this work, we have developed novel antimicrobial hydrogels composed of BC and the antimicrobial poly(3-hydroxy-acetylthioalkanoate-*co*-3-hydroxyalkanoate) (PHACOS). Hydrogels based on different PHACOS contents (20 and 50 wt%) were generated and analysed through different techniques (IR, DSC, TGA, rheology, SEM and EDX) and their bactericidal activity was studied against *Staphylococcus aureus*. PHACOS20 (BC 80%-PHACOS 20%) hydrogel shows mechanical and thermal properties in the range of human skin and anti-staphylococcal activity (kills 1.8 logs) demonstrating a huge potential for wound healing applications. Furthermore, the cytotoxicity assay using fibroblast cells showed that it keeps cell viability over 85% in all the cases after seven days.

© 2020 The Authors. Published by Elsevier B.V. This is an open access article under the CC BY license (http://creativecommons.org/licenses/by/4.0/).

1. Introduction

Some microorganisms naturally produce a huge variety of biopolymers such as polysaccharides, polyesters, and polyamides. These biopolymers present a renewable character, intrinsic biocompatibility, biodegradability and specific features [1], which make them good candidates for the development of biomaterials. In this work, bacterial cellulose (BC) and poly(3-hydroxy-acetylthioalkanoate-*co*-3-hydroxyalkanoate) biopolymer (PHACOS) were specifically chosen for the development of gels with antimicrobial properties for wound healing [2].

BC is a homopolymer produced by some bacterial strains [3] whose chemical structure is composed of linear chains of β-1,4-glucan that, in contrast with plant-derived cellulose, BC is free of lignin and hemicellulose. In addition, the degree of polymerization, is higher in BC [4] which has also influence on its mechanical properties. It has been demonstrated that BC regenerated from ionic liquids (e.g. BMIMCI) maintains the degree of polymerization, and polydispersity respect to those of the initial one. However, its morphology is significantly changed and its microfibrils are fused into a relatively homogeneous macrostructure. It has been demonstrated that the degree of crystallinity of the cellulose can change during its regeneration and, depending on the different regeneration conditions, the crystallinity of cellulose varies from crystalline to amorphous states [5]. Other advantage of BC is that it is a renovable polymer that can be produced by some bacterial strains [3].The highly pure 3-D structure of the nanofibers (3–8 nm) is stabilized by inter- and intra-fibrillar hydrogen bonds providing BC with unique mechanical characteristics [6]. It has a high tensile strength, mechanical stability, non-toxicity, high crystallinity, high water-holding capacity, a remarkable permeability to gases and liquids and a great compatibility with living tissues [7]. These intrinsic features make BC an ideal candidate for the preparation of wound dressings, especially for burn wounds, tissue regeneration and as temporary skin substitutes [8], as it provides a moist environment, an adequate gaseous exchange and thermal insulation, it is biocompatible, stable and presents low adherence to the skin [6]. Specifically, for wound healing applications,

* Corresponding authors at: Interdisciplinary Platform for Sustainable Plastics towards a Circular Economy-Spanish National Research Council (SusPlast-CSIC), Madrid, Spain.
E-mail addresses: mraguilar@ictp.csic.es (M.R. Aguilar), auxi@cib.csic.es (A. Prieto).

https://doi.org/10.1016/j.ijbiomac.2020.07.289
0141-8130/© 2020 The Authors. Published by Elsevier B.V. This is an open access article under the CC BY license (http://creativecommons.org/licenses/by/4.0/).

biocompatibility and water holding capacity have been modified in different ways [7]. Moreover, since BC lacks antimicrobial capacity, a very important property when considering skin burns treatments, most of the modifications have been driven to prevent microbial infections. Portela et al. reviewed the marketed BC-based wound dressing products and the materials used to reinforced BC, such as, among others, poly (vinyl alcohol) (PVA), that improves the mechanical properties, or chitosan and alginate, that enhance elongation, rehydration, swelling ratios and water vapour transmission, or silver nanoparticles, that confer antimicrobial activity [8].

Skin regeneration and wound healing involves several complex biological processes that attempt to restore the skin barrier function. Healing processes are specially delayed or impaired in those patients with underlying disorders that lead to chronic inflammation [9], or when the injure is infected, being *Staphylococcus aureus* and methicillin-resistant *Staphylococcus aureus* (MRSA) the most common cause of wound infection [10]. A review published in 2010 estimated that 150,000 patients were affected annually by MRSA infections in the European Union (EU), resulting in additional hospital attributable costs of EUR 380 million for EU healthcare systems [11]. Wound healing will be favoured if re-epithelization, connective tissue fibre regeneration and angiogenesis are promoted and infection is prevented [12].

Other bacterial biopolymer of biomedical interest are the polyhydroxyalkanoates (PHA) [13]. PHAs are hydrophobic polyesters of 3-hydroxyalkanoic acids stored as inclusions in the bacterial cytoplasm under nutrient limitations [14]. The side chain varies in length and composition, and depending on its length, PHA are classified as short chain length (scl) and medium chain length (mcl). Mcl-PHA can be tailored to the needs of specific applications by metabolic engineering and feeding specific bacterial species with structurally related carbon sources that are processed through the β-oxidation pathway [15]. PHACOS is a functionalized mcl-PHA produced in *Pseudomonas putida* [16]. This polymer contains monomers with thioester groups in the side chain that confer antibacterial activity to PHACOS specifically against *S. aureus* isolates including MRSA. PHACOS cellular toxicity in terms of viability and metabolic functions of mammalian cells were deeply studied by Dinjaski et al. Inflammatory activity was also analysed in vitro and in vivo by PHACOS implantation subcutaneously in mice. The results indicated minimal inflammation associated with this polymer [17].

Bactericidal hydrogels based on the combination of BC and mcl-PHA have not been reported so far. In this work, two biopolymers, BC and PHACOS were specifically chosen for the development of gels with antimicrobial properties for potential application in wound healing [2]. The good antimicrobial activity of PHACOS remained in the blend of these two biopolymers obtained from renewable sources. One of the main challenges of the present work was the dissolution of the BC and the incompatibility of both polymers, which was solved using ionic liquid as direct solvent. BC/PHACOS hydrogels with different proportions of the antimicrobial agent (20 and 50 wt%) were prepared, and the influence of PHACOS content on the structural features, morphology, and thermal and mechanical properties were deeply studied. Results were compared and discussed with non-bactericidal hydrogels based on BC and mcl-PHA containing 3-hydroxyoctanoic acid as major monomer (PHO) which were prepared under the same experimental conditions. Finally, the antimicrobial activity of the BC/PHACOS hydrogels was evaluated in vitro using *S. aureus* and their cytotoxicity assessed using fibroblasts of human embryonic skin.

2. Experimental

2.1. Materials

Poly(3-hydroxyoctanoate-*co*-3-hexanoate) copolymer with 5% of poly(3-hydroxyhexanoate) (hereafter called PHO), was a product from Bioplastech (Ltd Ireland). PHACOS was a bacterial functionalized polyester obtained from ADM-Biopolis, which monomer content was 40% of non-functionalized monomers (3-hydroxyoctanoate, 3-hydroxydecanoate, and 3-hydroxyhexanoate monomers) and 60% of functionalized monomers (3-hydroxy-6-acetylthiohexanoate and 3-hydroxy-4-acetylthiobutanoate monomers). BC pellicles were produced in static culture using the bacterial strain *Komagataeibacter medellinensis* ID13488 as previously described [18]. 1-Butyl-3-methylimidazolium chloride (BMIMCl) was purchased from Sigma-Aldrich and abcr GmbH.

2.2. Preparation of samples

Hydrogels were prepared by combination of different ratios of BC and PHACOS using a 1 wt/v-% of the total polymer concentration. The solubilization of the polymers was carried out following a protocol described by Hameed and col. [19] for plant cellulose and poly(3-hydroxybutyrate) (PHB) with the following modifications: To dissolve the BC, 235 mg of BC were mixed with 25 mL of BMIMCl (melted by heating at 70 °C), heated and stirred at 100 °C for 16 h to get a complete and homogeneous solution. To obtain a solution of PHACOS, about 235 mg were dispersed into 25 mL of BMIMCl. Both BC and PHACOS solutions were mixed in the desired proportions and stirred at 100 °C for another 16 h. The mixtures were poured into teflon moulds and coagulated in deionized water. The BMIMIC was removed by dialysis against water for 72 h. The dialysis time was established after verifying that the ionic liquid was completely removed from the sample using spectroscopic techniques. Finally, samples were frozen and lyophilized. Hydrogels of BC with PHO were obtained using the same methodology and tested as control as non-bactericidal hydrogels. Hydrogel samples with BC/PHACOS or BC/PHO 80/20 and 50/50 wt% ratios were obtained which were named as PHACOS20, PHO20, PHACOS50 and PHO50, respectively. BC was dissolved separately in the BMIMCl (melted by heating at 70 °C), heated and stirred at 100 °C for 48 h mimicking the hydrogels preparation conditions. Then, BC was subsequently regenerated in deionized water giving the product named as rBC (regenerated BC).

2.3. Characterization

2.3.1. ATR-FTIR analysis

Attenuated total internal reflectance Fourier transform infrared (ATR-FTIR) characterization of the hydrogels was carried out in a Perkin–Elmer (Spectrum One) spectrometer equipped with a ATR accessory. Spectra were recorded in the range from 4000 to 400 cm^{-1} by 32 scans and with a resolution of 4 cm^{-1}.

2.3.2. Thermogravimetric analysis (TGA)

Thermogravimetric analyses (TGA) of the hydrogels was performed on TGA Q500 (TA Instruments) thermogravimetric analyser, under dynamic nitrogen at a heating rate of 10 °C/min working in a range of 25–600 °C. Approximately, 10 mg of each dried hydrogel were weighed and the weight loss was recorded over temperature. The extrapolated onset temperature (T_{onset}), that denotes the temperature at which the weight loss starts, and temperature at peak maximum (T_{max}) in the DTG curve, that shows the maximum decomposition rate of a component of the material, were measured.

2.3.3. Differential scanning calorimetry (DSC)

Differential Scanning Calorimetry (DSC) was performed using a DSC8500 Perkin Elmer calorimeter. 5–10 mg of each dried sample were sealed in the pan and cooled to −70 °C at 20 °C/min, held for 5 min, and heated to 150 °C at 20 °C/min, and held at that temperature for 2 min to remove the thermal history. Then, the samples were cooled to −70 °C at 20 °C/min, held for 5 min and, finally, heated to 150 °C at 20 °C/min (second scan). As reference, an empty pan was employed. DSC was used to determine the glass transition temperature (T_g) values

which were taken as the midpoint of transition in the second scan of DSC thermograms.

2.3.4. Mechanical tests

The tensile behaviour of the hydrogels was analysed using a stress-controlled oscillatory rheometer ARG2 TA Instruments using parallel plate geometry. Hydrogels samples were measured using a cross hatched steel parallel plate (20 mm of diameter). The viscoelastic properties of the hydrogels were analysed examining their storage (G′) (elastic behaviour) and loss (G″) (viscous behaviour) moduli obtained in the dynamic mechanical analysis (stress-strain tests).

Strain sweeps were performed between 0.01 and 1000% strain, setting the normal force at 0.05 N with a frequency of 0.5 Hz. Frequency sweeps were done at 0.2% strain, 0.05 N normal force, from 0.1 to 100 Hz.

All hydrogels (80/20 and 50/50 BC/PHACOS and BC/PHO) were tested swollen in distilled water at 37 °C, using a rBC as control.

2.3.5. Scanning electron microscopy (SEM) and Energy dispersive spectroscopy (EDS)

The morphology of the freeze-dried hydrogels was examined by scanning electron microscopy (SEM) using a Hitachi SU8000 Field Emission Scanning Electron Microscope (FE-SEM) (Hitachi High-Technologies Corporation, Tokyo, Japan) with an accelerating voltage of 1 keV. Previous to the analysis, all samples were sputter-coated with gold (Polaron SC7640, Quorum Technologies Ltd., England). The elemental composition was determined by energy dispersive spectroscopy (EDS; Quantax 200, Bruker) coupled to SEM and data was processed and reported using the tools offered by ESPRIT software (Bruker, Germany).

2.3.6. Swelling studies

The swelling behaviour of hydrogels was studied in distilled water at room temperature (25 °C) and at different times. Firstly, the dried samples were weighed and, next, immersed in 10 mL of distilled water at room temperature. Then, the samples were taken from the solution at different time periods, wiped carefully with a filter paper and weighed. All the sample weights were taken in triplicate. The results are shown as percentage of swelling (%S) and calculated by the formula:

$$\%S = \frac{(W_t - W_d)}{W_d} \times 100$$

where W_d is the initial weight of the dried sample and W_t is the weight of the swollen sample at time *t*.

2.4. Antimicrobial assay

We design a new antimicrobial assay based on the JIS L 1902:2008-Absorption method [20] for testing the antimicrobial capacity of the biomaterials. It considers the microorganisms included in the matrix of the hydrogels and consists in the enzymatic depolymerisation of the material for releasing the bacterial cells just before the survival analysis.

S. aureus CECT 86 was grown in NB medium (Nutrient Broth Difcto™). Isolated bacterial colonies were subsequently inoculated into liquid NB medium and cultured at 37 °C under shaking conditions for 16 h. Bacterial concentration was estimated by optical density at 600 nm wavelength (OD_{600}), using a spectrophotometer (Ultrospec 10 cell density meter; Amersham Biosciencies). Cells in stationary growth phase were collected by centrifugation (20 min, 2906 ×*g*, 4 °C) and diluted to a final OD_{600} of 1, in 1/500 diluted NB medium (dilution of the NB with sterilized water to a 500-fold volume). These conditions allow bacterial survival, but avoid cell proliferation during the assay.

BC-based hydrogels (rBC, PHACOS20, PHACOS50, PHO20, PHO50) were cut in slices (0.9 cm^3) and sterilized by UV light for 15 min on each side, in a *GelDoc™* Molecular Imager® (BioRad). These sterilized hydrogel slices were introduced into the wells of a 24 well-plate (Nunclon, Thermo-Scientific), and covered with 200 μL of the latter cell suspension in 1/500 NB, with a final estimated concentration per well of 1×10^8 CFUs. Cell suspensions in the absence of contact material were used as bacterial growth controls (t0 and t24 *S. aureus* samples). Growth control at t0 was plated in agar-LB plates and total viable cells were counted after 16 h of incubation at 37 °C. The 24 well-plate with the samples was incubated for 24 h at 37 °C and saturated atmosphere (>90%).

To release absorbed cells inside the hydrogel, a mix of two enzymes was used. Commercially available cellulase (C2730, Sigma-Aldrich); and the mcl-PHA depolymerase (PhaZ), from *Streptomyces exfoliatus* K10 DSMZ 41693 $PhaZ_{Sex2.}$ The number 2 means that the strain *S. exfoliatus* K10 has two depolymerases: # 1 is PHB depolymerase and # 2, which is the mcl-PHA depolymerase used in this work, produced in *Rodococcus* sp. T104 (pENVO) and purified as described previously [21]. An enzymatic mix solution (DepolMS) was formulated for total depolymerization and solubilization of the hydrogels. Optimal conditions for DepolMS resulted to be 35 μg of cellulase to 1 μg of $PhaZ_{Sex2}$, in a final volume of 500 μL Tris-HCl pH 6.0 and 1 h 30 min incubation time at 30 °C with soft shaking. Although these are not the optimal conditions for the enzymatic catalyst, they were established to maintain cell survival while materials were hydrolysed.

DepolMS was added to the wells containing the hydrogels and to a cell suspension without any in-contact material as control. Subsequently, the resulting suspensions were recovered and plated in agar-LB plates and total viable cells were counted after 16 h of incubation at 37 °C. The reported data were the averages of 3–5 independent samples performed in duplicates.

A schematic representation of the antimicrobial test is displayed in Fig. S1.

2.5. Cytotoxicity

Cytotoxicity was assessed using fibroblasts of human embryonic skin (HFB, Innoprot). The culture medium was Dulbecco's modified Eagle's medium with HEPES enriched with 4500 mg/L of glucose (DMEM, Sigma) and supplemented with 10% FBS, 200 mM L-glutamine, 100 μg/mL penicillin and 100 μg/mL streptomycin (complete medium). Thermanox® (TMX) discs were used as negative control.

Following the ISO 10993–5 standard Indirect, cytotoxicity of hydrogels was analysed using Alamar Blue assay (AB, Biorad), [22]. This assay measured the response of cells to hydrogel extracts collected at different times. Briefly, sterilized hydrogels were set in 5 mL of FBS-free supplemented DMEM at 37 °C. Aliquots of medium extracts were taken at 4 h, 1, 4 and 7 days under sterile conditions. Fibroblasts were seeded at a density of 90,000 cells/mL in complete medium in a 96-well culture plate. After 24 h of incubation, the medium was replaced with the corresponding extract and further incubated for 24 h. Afterwards, extracts were replaced with 100 μL of AB dye (10% AB solution in phenol red free DMEM medium) and plates were incubated at 37 °C for 3 h in the dark. Finally, absorbance was monitored at 570 nm and 600 nm using a microplate reader (Biotek Synergy HT). Medium without hydrogel extracts was used as control. Results were normalized to the control (TMX) and given as mean ± SD ($n = 16$).

2.6. Statistical analysis

All data from antimicrobial assay and cytotoxicity are presented as mean ± SD. One-way ANOVA was used to determine the significant difference at which statistical significance was reported when the *p*-value was less than 0.05. Statistical analysis was performed using GraphPad InStat version 7.0 (GraphPad software, San Diego, CA).

3. Results and discussion

3.1. Preparation of samples

Ionic liquids have been widely used during the last decade in the preparation of materials for different biomedical applications [23]. They are used to dissolve and functionalize, for example, simple sugars, cyclodextrins, cellulose and polysaccharides, such as starch, chitin/chitosan, xylan, etc., or proteins, like silk [24,25]. The toxicity of this type of solvents has been questioned and a debate on their use on biomaterials science was open [26]. In recent years alternative new non-toxic and biodegradable bio-ionic liquids are being developed [27,28]. Traditional ionic liquids are also used on the preparation of biomaterials as long as the purification of the final product ensures the complete removal of the solvent [23,29–31].

In this work, BC and PHA blends were obtained by the dissolution of the polymers in BMIMCl and coagulation of the mixture in water. BMIMCl was used due to its ability to dissolve polymers of very different hydrophilicity (i.e., hydrophilic BC and hydrophobic PHACOS) and to disrupt intra- and intermolecular bonds of BC. [2,19,32–34]. Its high chloride concentration is highly effective in breaking the extensive network of hydrogen bonds, allowing the dissolution of higher concentrations of BC than other traditional systems, including non-derivatizing (organic liquid/inorganic salt, like *N,N*-dimethylacetamide/LiCl; or organic liquid/amine/SO_2, such as dimethylsulfoxide/trimethylamine/SO_2; or ammonia/ammonium salt; or aqueous bases, like 10% NaOH) and derivatizing solvents (CF_3COOH, HCOOH, *N,N*-dimethylformamide/N_2O_4) [35–37]. Dissolved BC in BMIMCl instantly coagulates in the presence of anti-solvents, such as water, methanol, ethanol, acetone, dichloromethane, acetonitrile, or mixtures of them [38]. Usually, higher degree of crystallinity is obtained when the BC is coagulated in deionized water, resulting in higher strength of the regenerated matrix [32]. Thus, application of this methodology allowed the preparation of bacterial biopolymers-based hydrogels containing the PHACOS polyhydroxyalkanoate. Purification of the systems was confirmed by ATR-FTIR spectroscopy. Fig. S2 shows the ATR-FTIR spectra for both PHA containing hydrogels along with that of ionic liquid. It can be clearly observed that the signals of BMIMCl at 3090 cm^{-1}, assigned to –C–H stretching band of the $–CH_2$ and $–CH_3$ stretching vibrations of the alkyl groups located at the nitrogen atoms of the imidazolium ring, and the bands at 1560 and 1466 cm^{-1}, that corresponds to the skeleton vibrations of the imidazole ring, disappeared in the spectra of all hydrogels [39]. Hydrogels of BC/PHACOS and BC/PHO blends with compositions 100/0, 80/20 and 50/50 (wt/wt) were obtained and thoroughly characterized as described in the following sections.

3.2. Structural characterization

FTIR was applied for the identification of BC polymorphs in celluloses of different origin. Nelson and O'Connor identified two forms of the cellulose (I and II) with specific infrared spectral bands depending on the contribution of the polymorphs of crystalline cellulose [40]. More recently, it was reported two forms of cellulose I (Iα and Iβ) in BC produced by the bacteria *Komagataeibacter medellinensis* by FTIR [41–45]. Cellulose II was also identified in the BC produced by *Acetobacter xylinum* [46] that is able to produce the two forms of cellulose, cellulose I and cellulose II.

FTIR was applied for the characterization of the *Komagataeibacter medellinensis* ID13488 cellulose [45]. Moreover, the effect of the treatment with ionic liquids on the cellulose structure was also studied. Table 1 summarizes the assignment of most important ATR-FTIR peaks of BC and rBC samples whose spectra are shown in Fig. 1.

The bands at 1427, 1281, 1205, 1157, 897, 745 and 708 cm^{-1} were attributed to cellulose I. The peak at 1427 cm^{-1} is normally reported at 1420 for cellulose II, but moves to higher wavenumbers depending on the content of cellulose I.

Table 1
Assignments of ATR-FTIR bands of *K. medellinensis* BC; abbreviations: ν: stretching; β: in-plane bending; ω: wagging; as: asymmetric; s: symmetric.

Frequency (cm^{-1})	Assignment	Cellulose I	Cellulose II
3341	ν(OH)	✓	✓
2901	ν(CH)	✓	✓
1642	OH of water absorbed from cellulose	✓	✓
1466	β(OH)	✓	✓
1427	$\beta_s(CH_2)$	✓	
1335	β(OH)		✓
1315	ω(CH_2)		✓
1281	β (CH_2)	✓	
1205	β(OH)	✓	
1162	ν_{as}(COC)		✓
1056	ν(CO)	✓	✓
1031	ν(CO)	✓	✓
897	Group C1 frequency	✓	
745	Iα		
708	Iβ		

Bands assigned to cellulose II were also identified in the *Komagataeibacter medellinensis* ID13488 BC. The high intensity bands at 1335 and 1315 cm^{-1} and the peak at 1162 cm^{-1}, that correspond to the C-O-C asymmetric stretching, are characteristics of cellulose II.

The peaks at 1056 cm^{-1} and 1031 cm^{-1} are associated to the C—O stretching and common to both polymorphs. These peaks are ascribed to the glycosidic C—H deformation with ring vibration contribution and O—H bending, which is typical from β-glycosidic linkages between cellulose in glucose.

The peaks at 745 and 708 cm^{-1} indicated the presence of both allomorphs (Iα and Iβ), respectively [41,42].

BC and rBC ATR-FTIR spectra were rather similar however, the rBC peaks were smoother. The main differences were observed in peaks at 1427, 1335, 1315, 1157, 1059, 1035 and 897 cm^{-1}. The peak at 1427 cm^{-1} of BC was less defined in the rBC spectrum, indicating an increase in amorphous cellulose. The bands of BC at 1335 and 1315 cm^{-1}, were not observed in the rBC spectrum in which only one peak appeared at 1318 cm^{-1}, that indicates again the presence of amorphous cellulose. The band assigned to the C-O-C asymmetric stretching moved from 1162 cm^{-1} to 1157 cm^{-1} and the two peaks at 1059 and 1035 cm^{-1} of the BC, which are associated to the C—O stretching,

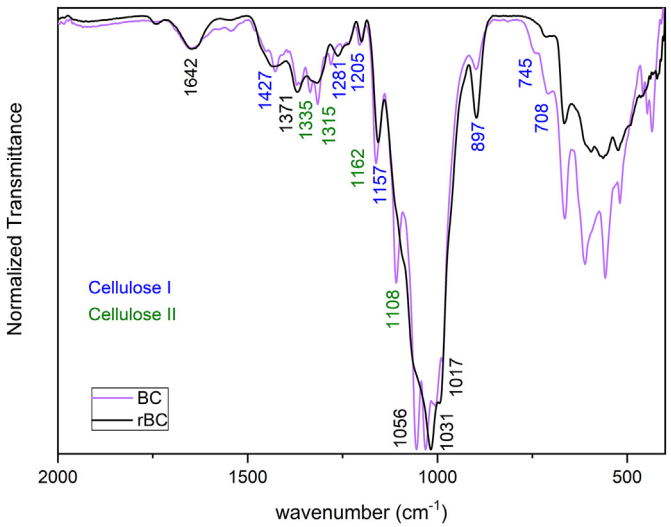

Fig. 1. ATR-FTIR bands of BC and rBC produced by *Komagataeibacter medellinensis* ID13488.

moved to a unique band at 1017 cm^{-1} in the case of the rBC. Moreover, the band at 897 cm^{-1} is higher in the case of rBC, which is associated with cellulose I. These changes corroborate that the treatment with the ionic liquid affects the crystallinity of the cellulose, as described previously [44], observing a higher contribution of cellulose I and amorphous cellulose in rBC.

Analysing the PHACOS hydrogels ATR-FTIR spectra (Fig. 2a), two peaks were observed for the carbonyl groups, one at 1734 and the other at 1691 cm^{-1}. The peak at 1734 cm^{-1} can be assigned to the carbonyl of the ester group (Fig. S3), and the band at 1691 cm^{-1} can be attributed to the thioester group. In both compositions a displacement to higher wavenumbers of these bands was observed with PHACOS content (1738 and 1693 cm^{-1} for PHACOS50, and at 1741 and 1694 cm^{-1} for PHACOS20), indicating that both carbonyl groups forms hydrogen bonds with BC in the hydrogels. In Fig. 2b, a schematic representation of the hydrogen interactions between BC and PHACOS is shown as previously reported by Hammed et al. for blends of cellulose and poly(3-hydroxybutyrate-*co*-3-hydroxyvalerate) (PHBV) [19].

Accordingly, in the FTIR spectra of non-bactericidal PHO hydrogels (Fig. S3) the carbonyl band at 1726 cm^{-1} moved to higher wavenumber in the spectra of PHO20 and PHO50 (1738 cm^{-1} and 1739 cm^{-1}, respectively) respect to PHO, due to intermolecular hydrogen bonding between cellulose and PHO [19]. The intensity of this band also increased as a function of PHO content.

Elemental analysis of PHACOS hydrogels was obtained by EDS and spectra of PHACOS20 and PHACOS50 are shown in Fig. S3. In both spectra, a peak at 2.15 keV corresponding to sulphur was shown that increased with PHACOS content. The absence of the band due to chlorine confirmed the proper elimination of the ionic liquid. The elements composition was 54.19 wt% of C, 44.11 wt% of O and 1.71 wt% of S in the case of PHACOS50, and 49.79 wt% of C, 49.95 wt% of O and 0.26 wt% of S for PHACOS20. These results confirmed the purification of the samples and corroborated the incorporation and entrapment of PHACOS within both hydrogel compositions.

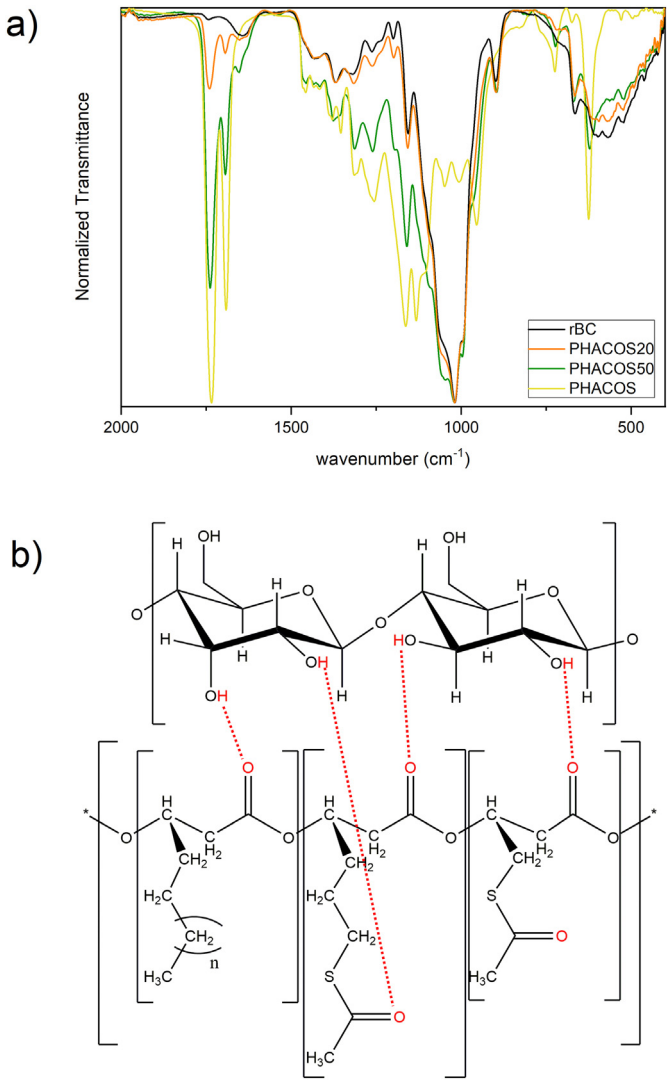

Fig. 2. a) ATR-FTIR bands of rBC, biopolymer PHACOS and BC/PHACOS blends of different composition. b) Possible hydrogen bonding interaction between BC and PHACOS.

3.3. Morphology

The morphology of lyophilized hydrogels was examined using SEM. Firstly, the surfaces of BC and the rBC were analysed and compared (Fig. 3a and b). As described previously [34,42,44], SEM micrographs of BC showed fibers of 50 nm diameter. However, this morphology significantly changed when analysing rBC; 50 nm fibers were still observed, but most of them were fused [19].

SEM micrographs of the PHA hydrogels blends showed characteristic phase separation structure of granules homogeneously dispersed in a porous BC matrix. The amount of granules increased as a function of PHA concentration. Surfaces with low content of PHA (20%) presented spherical beadlike microphase whereas those with higher PHA contents (50%) reflected smaller microdomains which appeared fused or very close to one others. Previous studies on blends of cellulose and PHBV reported similar findings [19]; the authors also observed that when PHBV was dissolved alone in BMIMCl it regenerated into a beadlike structure in the coagulation process. Accordingly, in our work, BC and PHAs were both completely dissolved in the ionic liquid forming a homogeneous solution in which the intermolecular hydrogen bonds of BC are broken and in turn, new hydrogen interactions between the polysaccharide and the corresponding PHA are formed as observed in the FTIR spectra of the lyophilized PHACOS hydrogels. Then, it can be assumed that phase separation takes place during the coagulation process in water and the microdomains are due to the corresponding PHA present in the formulation. These microdomains will participate in the hydrogen bonds with the hydroxyl groups of BC previously formed in the mixing solution. These type of interactions do not ensure a robust crosslinking, fact that is beneficial for the antimicrobial action of PHACOS. The exposure and availability of the PHACOS granules on the surface will favour the contact of the polyhydroxyalkanoate with bacteria wall, factor that is crucial to guarantee the antimicrobial activity of the system specially in infected wound healing.

Another relevant issue in tissue regeneration is porosity. Likewise, porosity of a hydrogel scaffold is very important for application in wound healing processes since it is associated with transport of nutrients and small molecules, and communication with biological moieties [47]. In this work, porosity of hydrogels showed an inhomogeneous pore distribution throughout the surface and it somewhat depended on PHA content. The influence of porosity of BC hydrogels on cell proliferation has been deeply investigated. Some studies supported that the inhomogeneous distribution of pores in the range 20–100 nm is not an advantage for cell proliferation. However, other recent papers reported a better performance of BC in wound dressing when the system was applied by its porous side compared to the more compact side [7]. In this context, some studies have been focused to optimizing the microporosity of bacterial cellulose scaffold using different kinds of porogens [48]. In our case, porosity of developed hydrogels was obtained by lyophilisation applying a conventional cycle. However, if needed, porosity could be adjusted by applying different freezing cycles [49]. Taking in overall the features of the PHACOS hydrogels, on the one side, porous bacterial cellulose will allow transport functions and on the

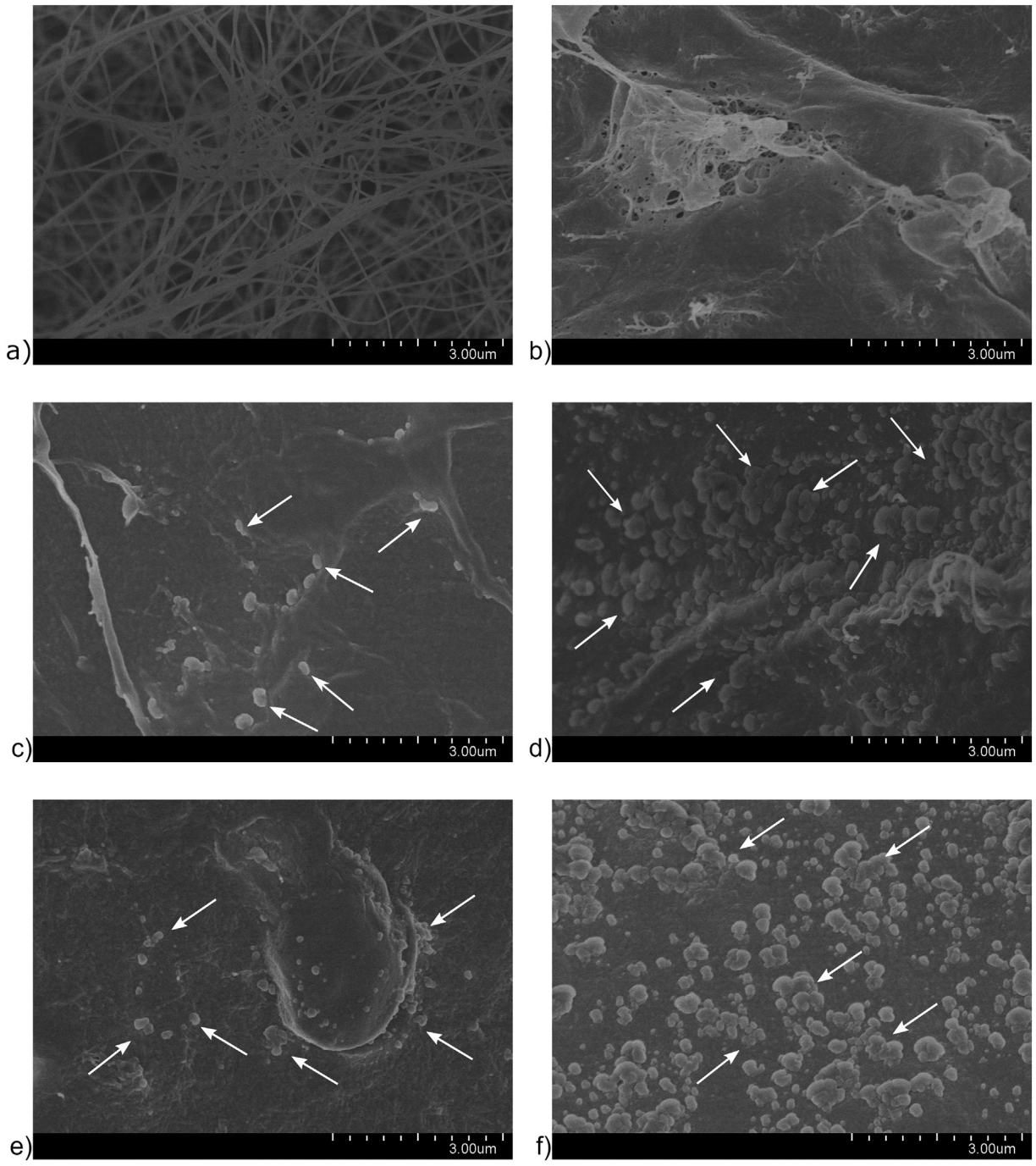

Fig. 3. SEM images (SU8000 3 kV) of a) BC; b) rBC; c) PHO20; d) PHO50; e) PHACOS20; and f) PHACOS50 samples.

other side, the distribution of the PHACOS beads over the surface matrix will promote antimicrobial action of the polyhydroxyalkanoate.

3.4. Thermal properties

Changes in heat capacity of hydrogels were obtained from their DSC thermograms which are displayed in Fig. S5. Thermograms showed the amorphous character of the blend hydrogels. Apparent glass transition was only detected for the PHA hydrogels containing 50 wt% of polyester. This can be an indication of the partial miscibility of the BC/PHA blends at lower content of the respective polyhydroxyalkanoate. Table 2 summarizes the obtained glass transition temperature values (T_g) of the blends containing 50% PHA. The T_g values were lower than those of initial PHAs, respectively. No crystallinity of the PHA was observed in any thermogram.

Thermal stability was analysed by thermogravimetry and main thermogravimetric parameters are summarized in Table 3. This technique is

Table 2
Summary of the T_g data of PHA hydrogels and initial PHA.

Sample	T_g (°C)
PHACOS	−30.43
PHACOS50	−38.11
PHO	−36.75
PHO50	−42.19

Table 3
TGA and DTG results of the PHA hydrogels and control samples.

	T_{onset} (°C)	T_{max1} (°C)	T_{max2} (°C)
BC	303	–	355
rBC	309	–	337
PHACOS	277	287	–
PHO	256	285	–
PHACOS20	269	288	325
PHACOS50	262	281	326
PHO20	261	280	342
PHO50	270	286	342

commonly used in the characterization of polymeric systems since it provides useful information on the intrinsic structure of the system. Thermal stability of rBC decreased if compared with native BC, as shown in Table 3. That is, T_{max} value decreased after the treatment with BMIMCl which can be attributed to a decrease in polymorph II and an increase in amorphous cellulose [34,44].

Thermal degradation of all hydrogel blends, underwent in two steps, presenting two maximum temperature (T_{max}) values in the DTG curves. The first weight loss was attributed to the PHAs thermal degradation whereas the second one was ascribed to the rBC pyrolysis. This degradation pattern indicates the not formation of interpolymeric matrix, it correlates with the segregation of the corresponding PHA within the cellulose matrix as observed in SEM examination and it is coherent with the amorphous state of the PHA within the hydrogels observed in DSC study.

On the other hand, since the proposed hydrogel system is intended to be used as a biomaterial for wound healing which is carried out at physiological temperature 37 °C, it can be said that the polymeric hydrogels will be thermally stable at that temperature.

3.5. Mechanical performance

Mimicking the mechanical properties of the skin is necessary in order to obtain a suitable hydrogel that do not damage the edges of the ulcer to be treated. Therefore, the mechanical properties of the new hydrogel must be adjusted in the same range as those of the skin to ensure better compatibility.

Viscoelastic properties of hydrogels swollen in water was carried out by means of rheological measurements.

The linear viscoelastic range (LVR) was determined between 0.01 and 5% strain (Fig. 4a); in this range the viscoelastic properties of all hydrogels were independent of the imposed strain levels but the PHACOS20 and PHO20 presented broader LVR. For strains values lower than 5%, G' was over G" in all hydrogels, which indicates that the samples have a gel-like structure. At strain levels higher that 10% the value of G' exceeds G", indicating that hydrogel structure was broken at that point.

rBC provided the highest storage modulus value, followed by PHACOS20 and PHO20 samples and the PHACOS50 and PHO50 gave the lowest. Therefore, adding polyesters to the bacterial cellulose produced a reduction in the storage modulus that can be attributed to the formation of new hydrogen interactions between both types of biopolymers, decreasing the intrinsic hydrogen bonds interactions of BC [50].

The frequency sweeps results revealed the dependence of the three dimensional structure of the hydrogels on the angular frequency (ω) as it is shown in Fig. 4b and Table 4. In the Fig. 4b it can also be appreciated that at high angular frequency values, between 100 and 300 rad/s, the structure of the hydrogels is not stable [51–53].

The highest G' value corresponds to the PHACOS20 hydrogel, followed by PHO50. The lowest values of G' were registered for PHACOS50 and PHO20. That is, PHACOS20 and PHO50 have a similar behaviour. Thus, in the case of the PHO, a 50 wt% of this polymer is necessary for getting a stable structure, but in the case of the PHACOS, only a 20% of the polymer is required. Analysing the structure of both PHAs,

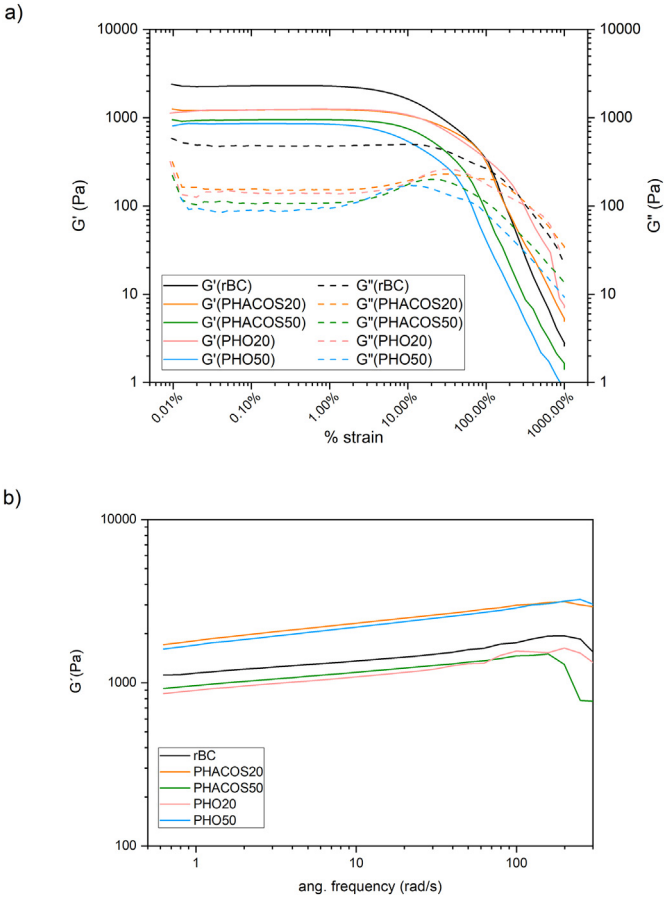

Fig. 4. a) Variation of storage modulus of hydrogels applying strain sweeps, and b) frequency sweeps.

PHACOS contains thioester groups at the end of the side chain that contribute to the formation of hydrogen bonds to stabilize the framework structure. However, as this type of carbonyl groups does not exist in PHO, higher amount of this polymer is needed to obtain a comparable storage modulus.

There is a wide range of elastic (G') and viscous (G") moduli reported in literature through different measurements (torsional, uni- or bi-axial). Holt et al. measured the viscoelastic response of whole human skin and dermis-only subjected to low-magnitude shear loads over a range of physiological frequencies (0.628 to 75.39 rad/s), similar to our conditions. They found that G' in whole skin increased over this frequency range from 325.0 ± 93.7 Pa to 1227.9 ± 498.8 Pa and dermis-only showed a similar trend with mean G' values increasing from 434.9 ± 122.1 to 6620.0 ± 849.5 Pa. Taking into consideration this work and analysing results of Fig. 4b and Table 4, our data show an increase of G' with ω less marked than that reported by Holt, however, G' values still lie in the range of those reported by skin and dermis-only samples [54], making these materials promising for the development of new wound dressings with antibacterial properties.

Table 4
Values of storage modulus (G') at three representative physiological angular frequencies.

	G' (Pa)		
	0.628 rad/s	0.99 (rad/s)	79.10 (rad/s)
rBC	1061.5 ± 77.1	1090.5 ± 79.9	1688.5 ± 53.0
PHO20	867.4 ± 36.1	908.0 ± 39.9	1427. 7 ± 41.1
PHO50	1571.0 ± 46.5	1663.7 ± 49.9	2689.3 ± 93.41
PHACOS20	1682.7 ± 80.2	1793.5 ± 100.2	3006.3 ± 396.91
PHACOS50	1056.0 ± 129.7	1111.6 ± 145.6	1694.5 ± 242.61

3.6. Swelling studies

The swelling capacity of a hydrogel is a critical and effective parameter for wound infection control because during the healing process fast and large water uptake capacity is needed to absorb exudates. In this sense, BC and its composites have been widely used in wound healing applications due to their high capability of water absorption.

Fig. 5 shows the water absorption capacity of each hydrogel developed in this work. It was observed that the swelling ability increased with time, first quickly and then gradually, reaching a constant swelling.

As it has been reported, BC has a strong swelling capacity in water due to the formation of multiple hydrogen bonds predominantly with the accessible hydroxyls groups in the amorphous regions of the polysaccharide [55]. The dissolution of BC in ionic liquid and subsequent regeneration to obtain rBC reduces significantly the crystallinity of the original material (as explained in Subsection 3.2), being the amorphous regions more accessible to water and leading to a higher swelling ratio.

PHACOS20 and PHO50 showed rather similar and remarkably high swelling potential compared to rBC alone. It could be ascribed to the presence of hydrophilic groups (-OH, -COO-, -$SCOC_3H$) that facilitates hydrogen bonding formation and favours water absorption. A similar parallelism between samples of these compositions was previously observed in their mechanical behaviour. PHACOS20 included 20% of PHA while PHO50 included 50%. PHACOS presents thioester groups at the end of the side chain that contribute to the formation of hydrogen bonds that further stabilize the structure if compared with PHO that needed to be included in higher concentration to achieve similar results.

In contrast, PHACOS50 resulted in the lowest water content, and it could be due to the formation of a more rigid hydrogel structure and the presence of a high amount of PHACOS granules at the surface (see Fig. 3) that hinders water absorption. Therefore, the amount of PHACOS present in the hydrogel is crucial to control the swelling ratio.

3.7. Antimicrobial activity

An effective wound dressing should ensure drainage and epithelial growth. During the wound healing process, dead tissue covers the wound and serves as a medium for bacterial growth, reduces the host's resistance to infection, delays the formation of granulation tissue and the re-epithelialization [56]. In this sense, the main goal of the present work was the development of novel bactericidal BC hydrogels that incorporate the polyhydroxyalkanoate PHACOS which has antimicrobial properties against S. aureus.

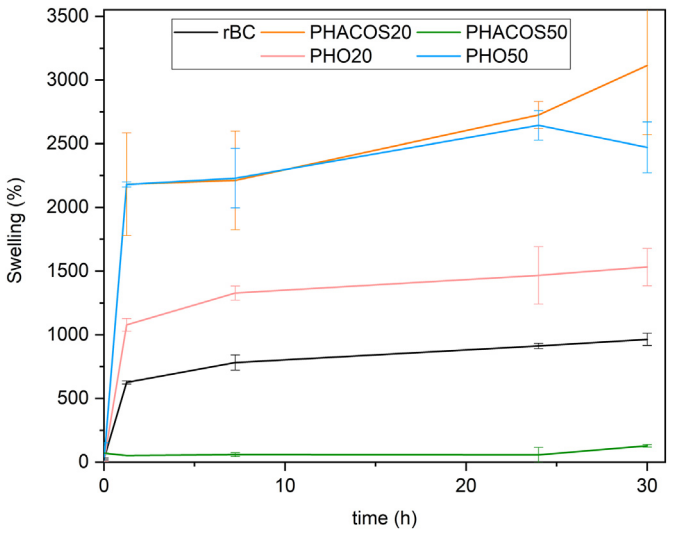

Fig. 5. Swelling profiles of hydrogels at different time periods.

The minimal inhibitory concentration (MIC) and the antimicrobial capacity of PHACOS has been reported in our previous articles [17,57]. We demonstrated the PHACOS antibacterial activity according to the ISO 22196:2011 for measurement the antibacterial activity on the plastic surface. We also calculated the MIC for the soluble oligomers and monomers released for the enzymatic hydrolysis of PHACOS and PHO as control, resulting in a much lower value for PHACOS (40 μM) than that of PHO (3 mM) [57]. In addition, the specificity of PHACOS against S. aureus strains, including MRSA clinical isolates, was fully demonstrated when compared to PHO in antimicrobial assays against a panel of 7 Gram-positive strains and 2 Gram-negative strains (including E. coli) [17].

The bactericidal behaviour of all prepared hydrogels in this work was analysed consequently against S. aureus.

Due to the great variety of antimicrobial applications, several standard methods to assess their efficiency have been developed. The most important standard antimicrobial methods for antibacterial hydrogels includes both qualitative (i.e. AATCC 147:2004, ISO 20645:2004) and quantitative (i.e. AATCC 100:2004, JIS L 1902:2008-Absorption method) methods. However, there is no consensus on the most adequate method to be used, and it is difficult to compare the data among them. BC-based hydrogels are porous materials with high water content. Taking into consideration that bacteria can colonize the whole structure, in this work the bactericidal assay was performed by applying a tailored methodology based on JIS L 1902:2008-Absorption method but suitable to assess the total bacterial load, including that absorbed or adhered inside the hydrogel in each tested condition. This method is based on the enzymatic hydrolysis of the biological polymers BC, PHACOS and PHO (for details see M&M 2.4, Fig. S1).

The bactericidal activity results against *S. aureus* is shown as the logarithmic difference between the number of bacteria in a control cell suspension (*S. aureus* t24) and each hydrogel-treated sample. Control shows that the viability of *S. aureus* was not significantly reduced due to incubation time and growth conditions, or when exposed to cellulase and PHA depolymerase (DepolMS) (Fig. 6a). Neither regenerated cellulose, nor hydrogels of BC-PHO, PHO20 and PHO50 displayed antibacterial activity, conversely to hydrogels containing PHACOS (Fig. 6a). PHACOS20 resulted in a cell viability decrease from 10^8 to 1.6×10^6, a 1.8 logarithmic unit reduction, and PHACOS50 decreased CFU from 10^8 to 1.6×10^5, a 2.8 logarithmic unit reduction, similarly to the antimicrobial activity reported in the literature for other hydrogels [58].These results show that the antibacterial behaviour of these BC-based hydrogels is due exclusively to the PHACOS component. Taking into account that direct contact is needed for the antibacterial activity, hydrogels may enhance bactericidal activity of PHACOS. It is important to notice that the specificity of PHACOS against *S. aureus*, far from being a drawback, restricted antibacterial activity over these important skin infecting bacteria. This is, in fact, considered an advantage, as it would leave unharmed commensal bacteria from the skin. *S. aureus* is a mayor skin pathogen. It is the main cause of impetigo, which accounts for 50–60% of all bacterial skin infections, and is also the main cause of cellulitis and folliculitis (skin infections). Moreover, PHACOS is active against MRSA [17] that may be responsible for up to 60% of skin infections seen in US emergency departments, reasons why we have targeted this microorganism. Our work also paves the way for further developments to design synergetic effective hydrogels containing for instance metal nanoparticles, biological extracts or antibiotics specific for other relevant skin infective bacteria (i.e. *Pseudomonas aeruginosa*).

Different strategies have been traditionally applied for conferring antimicrobial activity to hydrogels for wound healing [8]. The most conventional consists of loading antibiotics into the hydrogel as delivery system. Antibiotic treatment is one of the main approaches of modern medicine which is used to combat infections [60]. However, the emergence, spread, and persistence of multidrug-resistant (MDR) bacteria such as MRSA, advise against the misuse of antibiotics and raise demands for safe and efficacious agents that were less prone to

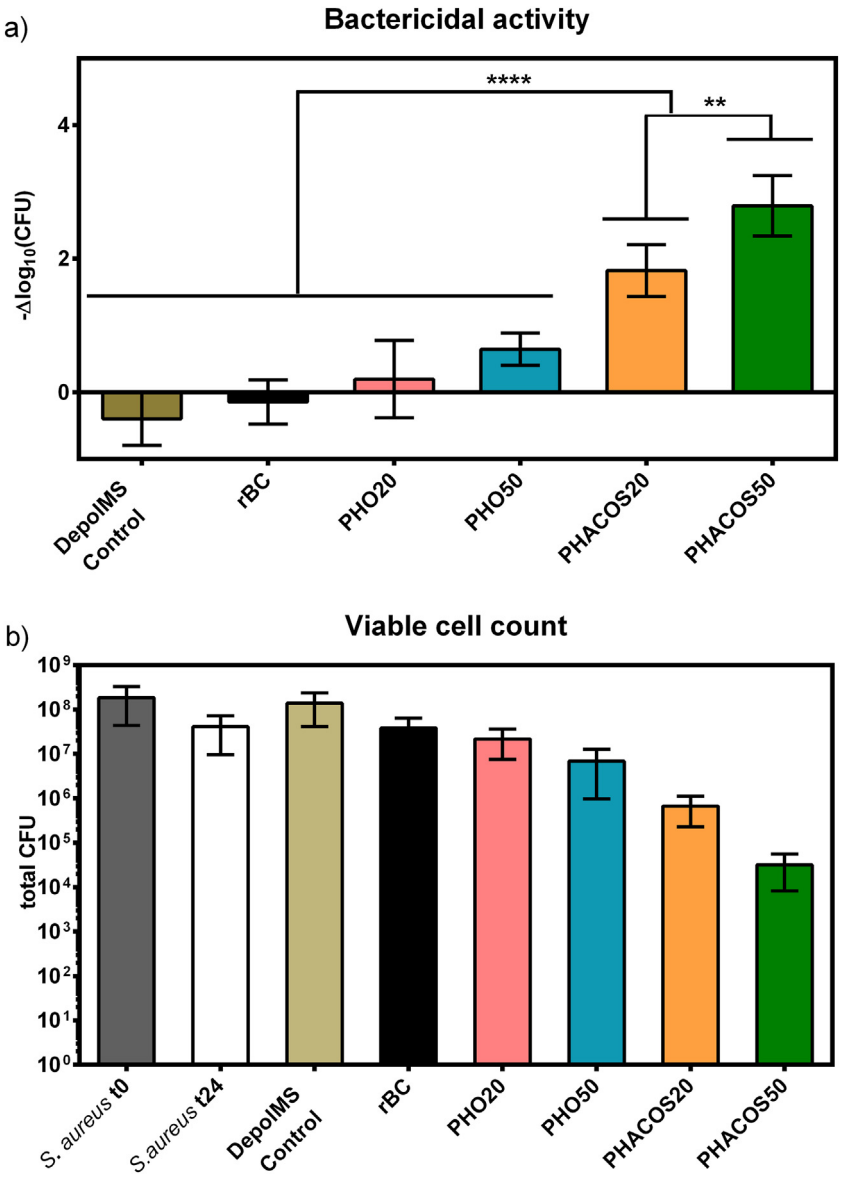

Fig. 6. Antimicrobial activity of the blended hydrogels. a) Logarithmic reduction of bacteria count for the suspension incubated with each hydrogel, regarding a cell suspension of *S. aureus* control. DepolMS refers to the suspension incubated with the enzymes; rBC with the regenerated cellulose; PHACOS20, PHACOS50, PHO20 and PHA50 with the corresponding hydrogel. Statistically significant differences from a one way ANOVA test are indicated with ** ($p < 0.01$) **** ($p < 0.0001$). b) Viable cell count from panel A.

stimulating development of resistance. In recent years, alternatives such as antimicrobial nanoparticles (e.g., Ag, ZnO or TiO2) and antimicrobial peptides (AMPs), have increased their attention [61], but these methodologies have some important limitations such as the maximum concentration that can be loaded within the polymer network. Natural polymers with inherent antibacterial properties like chitosan can overcome this issue, but its efficacy as pure polymers against certain important clinical isolated pathogen is scarcely reported [62]. In this work we have developed a new hydrogel with efficient antimicrobial activity against MRSA, using two natural bacterial biopolymers of different nature that can be produced by sustainable processes following the principles of circular economy including the reusability of the solvent applied for blending (ionic liquid).

3.8. Biocompatibility of hydrogels

Biocompatibility of BC with living tissues has been previously studied in repeated occasions and is comparable to other biomaterials commonly used in tissue engineering, like polyglycolic acid and polytetrafluorethylene [7]. BC is widely used in in vivo applications because it lacks proteins or polymers, a requirement of the United States food and drug administration (FDA) legislations for implants in direct contact with blood. In fact, several BC-based materials approved by the FDA are used as tissue surgical sheets, reinforcing matrixes and meshes, because of the absence of skin irritation and the lower coagulation rates compared to other materials [61]. Skin tolerance and in vivo response to BC applying skin lesion model, demonstrated that the erythema clinical score was zero at 2 and 24 h after patch removal in almost all volunteers [63. In vivo cytotoxicity of BC has been studied by implanting BC nanofibers subcutaneously in BALB/c mice, without showing changes in the normal development of animals [64].

PHACOS cellular toxicity in terms of viability and metabolic functions of mammalian cells were deeply studied by Dinjaski et al. Inflammatory activity was also analysed in vitro and in vivo by PHACOS implantation subcutaneously in mice. The results indicated minimal inflammation associated with this polymer [17].

Based on these antecedents, in this work, the cytotoxicity of antimicrobial BC/PHACOS hydrogels were evaluated according to ISO 10993-5

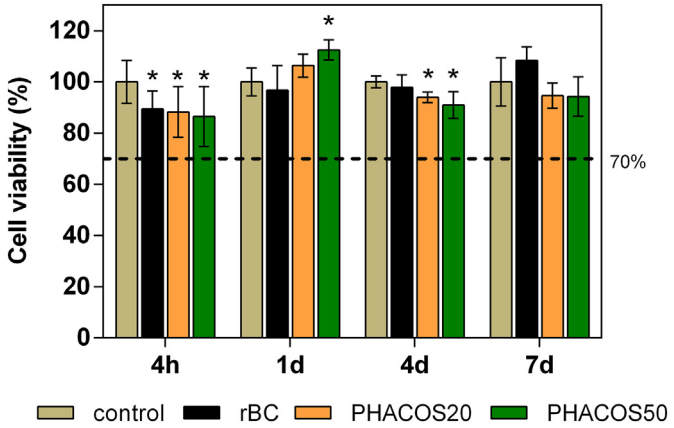

Fig. 7. Biocompatibility assay: Indirect cytotoxicity showing cell viability in the presence of extracts at different time points. Statistically significant differences between studied samples and control from a one way ANOVA test are indicated with * ($p < 0.05$).

standard using human dermal fibroblasts. Thus, the effects of material extracts on the metabolic activity of the cells were evaluated at different time periods. According to the standard, if the relative cell viability of the highest concentration of the sample extract (100% extract) is ≥70% of the control group, then the material shall be considered non-cytotoxic.

Fig. 7 shows cell viability (CV) values of human fibroblasts cultured in the presence of extracts of the PHACOS containing hydrogels samples taken at different time periods. It can be observed that cell viability in the presence of extracts of rBC and PHACOS hydrogels samples at 4 h was statistically lower than the control, however cell viability recovered in the presence of extracts taken in the following time points (1, 4 and 7) giving not statistically different values over the studied period except for some cases. Taking the results in overall, we can say that no sample showed cytotoxicity according to ISO 10993-5 standard since cell viability was over 85% in all studied samples.

4. Conclusion

Antimicrobial hydrogels based on BC and PHACOS were successfully prepared using the ionic liquid BMIMCl and were cytocompatible against fibroblasts of human embryonic skin. Hydrogels microstructure consisted in a BC matrix having PHACOS granules homogeneously distributed and stabilized by hydrogen bonding interactions between both types of polymers. The PHACOS20 had elastic properties comparable to the skin features, optimum swelling properties for absorbing fluids in wounds, and besides, presented the highest significant anti-staphylococcal activity (reduction of viability in 1.8 logarithmic units). 20% of PHACOS was enough to provide BC-based hydrogel with antimicrobial activity versus *S. aureus*, using low amount of polymer concentration in the synthesis (1 w/v-%). The hydrogel composition PHACOS20 is selected as the best candidate formulation and proposed for further developments in wound healing applications.

Supplementary data to this article can be found online at https://doi.org/10.1016/j.ijbiomac.2020.07.289.

Credit author statement

Virginia Rivero-Buceta: Conceptualization, Investigation, Writing - Original Draft, Visualization.

María Rosa Aguilar: Conceptualization, Supervision, Writing - Review & Editing. Corresponding author (2).

Ana María Hernández-Arriaga: Supervision, Writing - Original Draft.

Francisco G. Blanco: Investigation, Writing - Original Draft.

Antonia Rojas: Resources.

Marta Tortajada: Resources.

Rosa Ana Ramírez-Jiménez: Methodology.

Blanca Vázquez-Lasa: Supervision, Writing - Review & Editing.

Auxiliadora Prieto: Conceptualization, Supervision, Writing - Review & Editing Funding acquisition, Project administration. Corresponding author (1).

Acknowledgements

Authors thank financial support to thank the Spanish Ministry of Science, Innovation and Universities [MAT2017-84277-R and Bio2017-8344-8-R], the European Union's Horizon 2020 Research and Innovation Programme [grant agreement no 870294 (Mix-Up)] and the Community of Madrid [P2018/NMT4389] for the financial support of this project. The kind support by David Gómez in the SEM experiments is greatly appreciated.

References

[1] S.C.M. Fernandes, P. Sadocco, A. Alonso-Varona, T. Palomares, A. Eceiza, A.J.D. Silvestre, I. Mondragon, C.S.R. Freire, Bioinspired antimicrobial and biocompatible bacterial cellulose membranes obtained by surface functionalization with aminoalkyl groups, ACS Appl. Mater. Interfaces 5 (2013) 3290–3297, https://doi.org/10.1021/am400338n.

[2] J. Yang, J. Li, Self-assembled cellulose materials for biomedicine: a review, Carbohydr. Polym. 181 (2018) 264–274, https://doi.org/10.1016/j.carbpol.2017.10.067.

[3] A.F. Jozala, L.C. de Lencastre-Novaes, A.M. Lopes, V. de Carvalho Santos-Ebinuma, P.G. Mazzola, A. Pessoa-Jr, D. Grotto, M. Gerenutti, M.V. Chaud, Bacterial nanocellulose production and application: a 10-year overview, Appl. Microbiol. Biotechnol. 100 (2016) 2063–2072, https://doi.org/10.1007/s00253-015-7243-4.

[4] M. Tabuchi, K. Watanabe, Y. Morinaga, F. Yoshinaga, Acetylation of Bacterial Cellulose: Preparation of Cellulose Acetate Having a High Degree of Polymerization, vol. 42, 1998 1451–1454.

[5] S. Zhu, Y. Wu, Q. Chen, Z. Yu, C. Wang, S. Jin, Y. Ding, G. Wu, Dissolution of cellulose with ionic liquids and its application: a mini-review, Green Chem. 8 (2006) 325–327, https://doi.org/10.1039/b601395c.

[6] W. Czaja, A. Krystynowicz, S. Bielecki, R.M. Brown, Microbial cellulose - the natural power to heal wounds, Biomaterials 27 (2006) 145–151, https://doi.org/10.1016/j.biomaterials.2005.07.035.

[7] I. Sulaeva, U. Henniges, T. Rosenau, A. Potthast, Bacterial cellulose as a material for wound treatment: properties and modifications: a review, Biotechnol. Adv. 33 (2015) 1547–1571, https://doi.org/10.1016/j.biotechadv.2015.07.009.

[8] R. Portela, C.R. Leal, P.L. Almeida, R.G. Sobral, Bacterial cellulose: a versatile biopolymer for wound dressing applications, Microb. Biotechnol. 2019 (2019)https://doi.org/10.1111/1751-7915.13392.

[9] M.P. Rowan, L.C. Cancio, E.A. Elster, D.M. Burmeister, L.F. Rose, S. Natesan, R.K. Chan, R.J. Christy, K.K. Chung, Burn wound healing and treatment: review and advancements, Crit. Care 19 (2015) 1–12, https://doi.org/10.1186/s13054-015-0961-2.

[10] J.V. Vayalumkal, T. Jadavji, Children hospitalized with skin and soft tissue infections, Pediatr. Drugs 8 (2006) 99–111, https://doi.org/10.2165/00148581-200608020-00003.

[11] R. Köck, K. Becker, B. Cookson, S. Harbarth, J. Kluytmans, M. Mielke, G. Peters, R.L. Skov, Methicillin-resistant Staphylococcus aureus (MRSA): burden of disease and control challenges in Europe, Euro Surveill 15 (2010), 19688https://doi.org/10.2807/ese.15.41.19688-en.

[12] M.E. Aljghami, S. Saboor, S. Amini-Nik, Emerging innovative wound dressings, Ann. Biomed. Eng. 47 (2019) 659–675, https://doi.org/10.1007/s10439-018-02186-w.

[13] M. Zinn, B. Witholt, T. Egli, Occurrence, Synthesis and Medical Application of Bacterial Polyhydroxyalkanoate, vol. 53, 2001 5–21.

[14] A. Prieto, I.F. Escapa, V. Martínez, N. Dinjaski, C. Herencias, F. de la Peña, N. Tarazona, O. Revelles, A holistic view of polyhydroxyalkanoate metabolism in Pseudomonas putida, Environ. Microbiol. 18 (2016) 341–357, https://doi.org/10.1111/1462-2920.12760.

[15] M. Tortajada, L.F. da Silva, M.A. Prieto, Second-generation functionalized mediumchain- length polyhydroxyalkanoates: the gateway to high-value bioplastic applications, Int. Microbiol. 16 (2013) 1–15, https://doi.org/10.2436/20.1501.01.175.

[16] I.F. Escapa, V. Morales, V.P. Martino, E. Pollet, L. Avérous, J.L. García, M.A. Prieto, Disruption of β-oxidation pathway in Pseudomonas putida KT2442 to produce new functionalized PHAs with thioester groups, Appl. Microbiol. Biotechnol. 89 (2011) 1583–1598, https://doi.org/10.1007/s00253-011-3099-4.

[17] N. Dinjaski, M. Fernández-Gutiérrez, S. Selvam, F.J. Parra-Ruiz, S.M. Lehman, J. San Román, E. García, J.L. García, A.J. García, M.A. Prieto, PHACOS, a functionalized bacterial polyester with bactericidal activity against methicillin-resistant Staphylococcus aureus, Biomaterials 35 (2014) 14–24, https://doi.org/10.1016/j.biomaterials.2013.09.059.

[18] A.M. Hernández-Arriaga, C. del Cerro, L. Urbina, A. Eceiza, M.A. Corcuera, A. Retegi, M. Auxiliadora Prieto, Genome sequence and characterization of the bcs clusters for the production of nanocellulose from the low pH resistant strain

Komagataeibacter medellinensis ID13488, Microb. Biotechnol. 12 (2019) 620–632, https://doi.org/10.1111/1751-7915.13376.
[19] N. Hameed, Q. Guo, F.H. Tay, S.G. Kazarian, Blends of cellulose and poly(3-hydroxybutyrate-co-3-hydroxyvalerate) prepared from the ionic liquid 1-butyl-3-methylimidazolium chloride, Carbohydr. Polym. 86 (2011) 94–104, https://doi.org/10.1016/j.carbpol.2011.04.016.
[20] E. Pinho, L. Magalhães, M. Henriques, Antimicrobial Activity Assessment of Textiles: Standard Methods Comparison, 2011 493–498, https://doi.org/10.1007/s13213-010-0163-8.
[21] V. Martínez, P.G. de Santos, J. García-Hidalgo, D. Hormigo, M.A. Prieto, M. Arroyo, I. de la Mata, Novel extracellular medium-chain-length polyhydroxyalkanoate depolymerase from Streptomyces exfoliatus K10 DSMZ 41693: a promising biocatalyst for the efficient degradation of natural and functionalized mcl-PHAs, Appl. Microbiol. Biotechnol. 99 (2015) 9605–9615, https://doi.org/10.1007/s00253-015-6780-1.
[22] C.S.A. (CSA), Iso 10993-5, Int. Organ, vol. 2007, 2009 1–11, https://doi.org/10.1021/es0620181.
[23] S.S. Silva, T.C. Santos, M.T. Cerqueira, A.P. Marques, L.L. Reys, T.H. Silva, S.G. Caridade, J.F. Mano, R.L. Reis, The use of ionic liquids in the processing of chitosan/silk hydrogels for biomedical applications, Green Chem. 14 (2012) 1463–1470, https://doi.org/10.1039/c2gc16535j.
[24] O.A. El Seoud, A. Koschella, L.C. Fidale, S. Dorn, T. Heinze, Applications of ionic liquids in carbohydrate chemistry: a window of opportunities, Biomacromolecules 8 (2007) 2629–2647, https://doi.org/10.1021/bm070062i.
[25] J. Zhang, J. Wu, J. Yu, X. Zhang, J. He, J. Zhang, Application of ionic liquids for dissolving cellulose and fabricating cellulose-based materials: state of the art and future trends, Mater. Chem. Front. 1 (2017) 1273–1290, https://doi.org/10.1039/c6qm00348f.
[26] I.M. Marrucho, L.C. Branco, L.P.N. Rebelo, Ionic liquids in pharmaceutical applications, Annu. Rev. Chem. Biomol. Eng. 5 (2014) 527–546, https://doi.org/10.1146/annurev-chembioeng-060713-040024.
[27] T. Santos de Almeida, A. Júlio, N. Saraiva, A.S. Fernandes, M.E.M. Araújo, A.R. Baby, C. Rosado, J.P. Mota, Choline- versus imidazole-based ionic liquids as functional ingredients in topical delivery systems: cytotoxicity, solubility, and skin permeation studies, Drug Dev. Ind. Pharm. 43 (2017) 1858–1865, https://doi.org/10.1080/03639045.2017.1349788.
[28] J.M. Gomes, S.S. Silva, R.L. Reis, Biocompatible ionic liquids: fundamental behaviours and applications, Chem. Soc. Rev. 48 (2019) 4317–4335, https://doi.org/10.1039/c9cs00016j.
[29] R.F.P. Pereira, K. Zehbe, C. Günter, T. Dos Santos, S.C. Nunes, F.A.A. Paz, M.M. Silva, P.L. Granja, A. Taubert, V. De Zea Bermudez, Ionic liquid-assisted synthesis of Mesoporous silk fibroin/silica hybrids for biomedical applications, ACS Omega 3 (2018) 10811–10822, https://doi.org/10.1021/acsomega.8b02051.
[30] F. Lv, C. Wang, P. Zhu, C. Zhang, Characterization of chitosan microparticles reinforced cellulose biocomposite sponges regenerated from ionic liquid, Cellulose 21 (2014) 4405–4418, https://doi.org/10.1007/s10570-014-0440-y.
[31] S. Islam, L. Arnold, R. Padhye, Comparison and characterisation of regenerated chitosan from 1-butyl-3-methylimidazolium chloride and chitosan from crab shells, Biomed. Res. Int. 2015 (2015) 1–6, https://doi.org/10.1155/2015/874316.
[32] Z. Liu, X. Sun, M. Hao, C. Huang, Z. Xue, T. Mu, Preparation and characterization of regenerated cellulose from ionic liquid using different methods, Carbohydr. Polym. 117 (2015) 54–62, https://doi.org/10.1016/j.carbpol.2014.09.053.
[33] M.T. Clough, K. Geyer, P.A. Hunt, S. Son, U. Vagt, T. Welton, Ionic liquids: not always innocent solvents for cellulose, Green Chem. 17 (2015) 231–243, https://doi.org/10.1039/c4gc01955e.
[34] R.P. Swatloski, S.K. Spear, J.D. Holbrey, R.D. Rogers, Dissolution of cellose with ionic liquids, J. Am. Chem. Soc. 124 (2002) 4974–4975, https://doi.org/10.1021/ja025790m.
[35] M. Isik, H. Sardon, D. Mecerreyes, Ionic liquids and cellulose: dissolution, chemical modification and preparation of new cellulosic materials, Int. J. Mol. Sci. 15 (2014) 11922–11940, https://doi.org/10.3390/ijms150711922.
[36] T. Heinze, A. Koschella, Solvents applied in the field of cellulose chemistry: a mini review, Polímeros. 15 (2006) 84–90, https://doi.org/10.1590/s0104-14282005000200005.
[37] S. Wang, A. Lu, L. Zhang, Recent advances in regenerated cellulose materials, Prog. Polym. Sci. 53 (2016) 169–206, https://doi.org/10.1016/j.progpolymsci.2015.07.003.
[38] A.P. Dadi, S. Varanasi, C.A. Schall, Enhancement of cellulose saccharification kinetics using an ionic liquid pretreatment step, Biotechnol. Bioeng. 95 (2006) 904–910, https://doi.org/10.1002/bit.21047.
[39] F.A. Yassin, F.Y. El Kady, H.S. Ahmed, L.K. Mohamed, S.A. Shaban, A.K. Elfadaly, Highly effective ionic liquids for biodiesel production from waste vegetable oils, Egypt. J. Pet. 24 (2015) 103–111, https://doi.org/10.1016/j.ejpe.2015.02.011.
[40] M.L. Nelson, R.T. O'Connor, Relation of certain infrared bands to cellulose crystallinity and crystal lattice type. Part II. A new infrared ratio for estimation of crystallinity in celluloses I and II, J. Appl. Polym. Sci. 8 (1964) 1325–1341, https://doi.org/10.1002/app.1964.070080323.
[41] C. Molina-Ramírez, C. Castro, R. Zuluaga, P. Gañán, Physical characterization of bacterial cellulose produced by Komagataeibacter medellinensis using food supply chain waste and agricultural by-products as alternative low-cost feedstocks, J. Polym. Environ. 26 (2018) 830–837, https://doi.org/10.1007/s10924-017-0993-6.
[42] C. Molina-Ramírez, M. Castro, M. Osorio, M. Torres-Taborda, B. Gómez, R. Zuluaga, C. Gómez, P. Gañán, O.J. Rojas, C. Castro, Effect of different carbon sources on bacterial nanocellulose production and structure using the low pH resistant strain Komagataeibacter medellinensis, Materials (Basel) 10 (2017)https://doi.org/10.3390/ma10060639.
[43] F. Carrillo, X. Colom, J.J. Suñol, J. Saurina, Structural FTIR analysis and thermal characterisation of lyocell and viscose-type fibres, Eur. Polym. J. 40 (2004) 2229–2234, https://doi.org/10.1016/j.eurpolymj.2004.05.003.
[44] J.-H. Pang, X. Liu, M. Wu, Y.-Y. Wu, X.-M. Zhang, R.-C. Sun, Fabrication and characterization of regenerated cellulose films using different ionic liquids, J. Spectrosc. 2014 (2014) 1–8, https://doi.org/10.1155/2014/214057.
[45] L. Urbina, A.M. Hernández-Arriaga, A. Eceiza, N. Gabilondo, M.A. Corcuera, M.A. Prieto, A. Retegi, By-products of the cider production: an alternative source of nutrients to produce bacterial cellulose, Cellulose 24 (2017) 2071–2082, https://doi.org/10.1007/s10570-017-1263-4.
[46] J.R. Malcom Brown, Cellulose: structural and functional aspects (1989) 145–151.
[47] X. Zhang, Z. Li, X. Che, L. Yu, W. Jia, R. Shen, J. Chen, Y. Ma, G.Q. Chen, Synthesis and characterization of polyhydroxyalkanoate organo/hydrogels, Biomacromolecules 20 (2019) 3303–3312, https://doi.org/10.1021/acs.biomac.9b00479.
[48] M. Zaborowska, A. Bodin, H. Bäckdahl, J. Popp, A. Goldstein, P. Gatenholm, Microporous bacterial cellulose as a potential scaffold for bone regeneration, Acta Biomater. 6 (2010) 2540–2547, https://doi.org/10.1016/j.actbio.2010.01.004.
[49] S.V. Madihally, H.W.T. Matthew, Porous chitosan scaffolds for tissue engineering, Biomaterials 20 (1999) 1133–1142, https://doi.org/10.1016/S0142-9612(99)00011-3.
[50] J.D. Conrad, G.M. Harrison, The rheology and processing of renewable resource polymers, AIP Conf. Proc. 1027 (2008) 114–116, https://doi.org/10.1063/1.2964497.
[51] R. Shah, R. Vyroubal, H. Fei, N. Saha, T. Kitano, P. Saha, Preparation of bacterial cellulose based hydrogels and their viscoelastic behavior, AIP Conf. Proc. 1662 (2015) 1–8, https://doi.org/10.1063/1.4918895.
[52] P. Basu, N. Saha, P. Saha, Swelling and rheological study of calcium phosphate filled bacterial cellulose-based hydrogel scaffold, J. Appl. Polym. Sci. 48522 (2019) 48522, https://doi.org/10.1002/app.48522.
[53] Y. Numata, H. Kono, A. Mori, R. Kishimoto, K. Tajima, Structural and rheological characterization of bacterial cellulose gels obtained from Gluconacetobacter genus, Food Hydrocoll. 92 (2019) 233–239, https://doi.org/10.1016/j.foodhyd.2019.01.060.
[54] B. Holt, A. Tripathi, J. Morgan, Viscoelastic response of human skin to low magnitude physiologically relevant shear, J. Biomech. 41 (2008) 2689–2695, https://doi.org/10.1016/j.jbiomech.2008.06.008.
[55] S. Rongpipi, D. Ye, E.D. Gomez, E.W. Gomez, Progress and opportunities in the characterization of cellulose – an important regulator of cell wall growth and mechanics, Front. Plant Sci. 9 (2019) 1–28, https://doi.org/10.3389/fpls.2018.01894.
[56] I.S. Savitskaya, D.H. Shokatayeva, A.S. Kistaubayeva, L.V. Ignatova, I.E. Digel, Antimicrobial and wound healing properties of a bacterial cellulose based material containing B. subtilis cells, Heliyon 5 (2019)https://doi.org/10.1016/j.heliyon.2019.e02592.
[57] V. Martínez, N. Dinjaski, I.I. de Eugenio, F. de la Peña, M.A. Prieto, Cell system engineering to produce extracellular polyhydroxyalkanoate depolymerase with targeted applications, Int. J. Biol. Macromol. 71 (2014) 28–33, https://doi.org/10.1016/j.ijbiomac.2014.04.013.
[58] M.S. Kim, G.W. Oh, Y.M. Jang, S.C. Ko, W.S. Park, I.W. Choi, Y.M. Kim, W.K. Jung, Antimicrobial hydrogels based on PVA and diphlorethohydroxycarmalol (DPHC) derived from brown alga Ishige okamurae: an in vitro and in vivo study for wound dressing application, Mater. Sci. Eng. C. 107 (2020), 110352https://doi.org/10.1016/j.msec.2019.110352.
[60] W. Liu, H. Du, M. Zhang, K. Liu, H. Liu, H. Xie, X. Zhang, C. Si, Bacterial cellulose-based composite scaffolds for biomedical applications: a review, ACS Sustain. Chem. Eng. 8 (2020) 7536–7562, https://doi.org/10.1021/acssuschemeng.0c00125.
[61] G.F. Picheth, C.L. Pirich, M.R. Sierakowski, M.A. Woehl, C.N. Sakakibara, C.F. de Souza, A.A. Martin, R. da Silva, R.A. de Freitas, Bacterial cellulose in biomedical applications: a review, Int. J. Biol. Macromol. 104 ((2017) 97–106, https://doi.org/10.1016/j.ijbiomac.2017.05.171.
[62] E.M. Costa, S. Silva, F.K. Tavaria, M.M. Pintado, Insights into chitosan antibiofilm activity against methicillin-resistant Staphylococcus aureus, J. Appl. Microbiol. 122 (2017) 1547–1557, https://doi.org/10.1111/jam.13457.
[63] I.F. Almeida, T. Pereira, N.H.C.S. Silva, F.P. Gomes, A.J.D. Silvestre, C.S.R. Freire, J.M. Sousa Lobo, P.C. Costa, Bacterial cellulose membranes as drug delivery systems: an in vivo skin compatibility study, Eur. J. Pharm. Biopharm. 86 (2014) 332–336, https://doi.org/10.1016/j.ejpb.2013.08.008.
[64] R.A.N. Pértile, S. Moreira, R.M. Gil Da Costa, A. Correia, L. Guardão, F. Gartner, M. Vilanova, M. Gama, Bacterial cellulose: long-term biocompatibility studies, J. Biomater. Sci. Polym. Ed. 23 (2012) 1339–1354, https://doi.org/10.1163/092050611X581516.